should be completely excluded on the model. Therefore, transitions to bound states can be relied upon to account for the bulk of the β activity of Al^{25}.

It thus appears that all of the experimental data reported here fit well into a rotational picture with a nuclear deformation similar to that which fits the spectrum of low-lying states. More detailed knowledge of the relative $K = \frac{3}{2}^+$ purity of the $T = \frac{3}{2}$ states is necessary to determine if a single value of the deformation parameter can simultaneously explain all of the measured values.

It is tempting to try to apply this same picture to other cases—in particular to P^{29}. However, for mass 29 a clear-cut rotational description of the low-lying states

does not seem to be possible. Therefore, even if such a picture could be developed for the $T = \frac{3}{2}$ states, it would be difficult to test. Other cases may be more favorable but such have yet to be investigated.

ACKNOWLEDGMENTS

Pion Double-Charge-Exchange Cross-Section Measurements*

C. J. COOK,† M. E. NORDBERG, JR.,‡ AND R. L. BURMAN

Department of Physics and Astronomy, University of Rochester, Rochester, New York 14627

(Received 31 May 1968)

The differential cross section for the pion double-charge-exchange reaction $V^{51}(\pi^+,\pi^-)$, at an incident energy of 31 MeV and a production angle of 29°, has been measured to be $0.52_{-0.19}^{+0.71}$ μb/sr. The apparatus was sensitive to a pion-energy difference of 7 to 19 MeV, which covers the predicted isobaric analog state of $\Delta T_Z = 2$. A similar measurement for $Li^7(\pi^+,\pi^-)$ gave a differential cross section of $0.165_{-0.060}^{+0.225}$ μb/sr. Particle trajectories were photographed in thin-foil spark chambers. The charge and momenta of outgoing particles were determined with a magnet, and their range was determined in a thick-plate spark chamber.

I. INTRODUCTION

A PION double-charge-exchange reaction is a pion nuclear reaction of the type $\pi^{\pm} + (Z,N) \rightarrow \pi^{\mp} + (Z \pm 2, N \mp 2)$. A number of calculations and experiments relating to these reactions have been performed since 1963. It has been expected that these reactions might be useful in producing new nuclides with large excesses of neutrons or protons, in exciting isobaric analog states with $\Delta T_3 = \pm 2$, and in testing for correlations of nucleons within the nucleus.[1-5] These expectations are not yet experimentally well fulfilled.

Several theoretical estimates have been made of the double-charge-exchange cross section for low-energy incident pions. Kohmura predicted a total double-charge-exchange cross section of 15 μb for 10-MeV positive pions on O^{18}.[6] Kerman and Logan give tables which, when interpolated for 30-MeV pions on V^{51}, predict a total cross section of about 1 μb.[7] Parsons, Trefil, and Drell give a forward differential cross section for 30-MeV pions on O^{18} of about 0.06 μb/sr to the Ne^{18} analog state and about an equal cross section to other Ne^{18} excited states.[8]

The theory of Koltun and Reitan[9] predicts a large cross section at low energy. This theory uses a phenomenological single-charge-exchange Hamiltonian in second-order Born approximation. In the zero-energy limit, it gives an isotropic-differential cross section

$$d\sigma/d\Omega = 7.6(q'/q)|\langle f | T_+T_+ | i\rangle|^2 \ \mu\text{b/sr} \qquad (1)$$

for the reaction $\pi^+ \rightarrow \pi^-$. The T_+ is the nuclear isospin raising operator and the squared matrix element is equal to $(N-Z)(N-Z-1)/2$. Because of the raising operators, the final state should be an isobaric analog of the initial state with $\Delta T_3 = 2$. The q and q' are the initial and final pion momenta. They differ because of

[1] D. H. Wilkinson, Proc. Phys. Soc. (London) **80**, 997 (1962).
[2] T. Ericson, in *Proceedings of the 1963 Annual International Conference on High Energy Physics and Nuclear Structure at CERN* (CERN, Geneva, 1963).
[3] M. Jean, Nuovo Cimento Suppl. **2**, 400 (1964).
[4] S. Barshay and G. E. Brown, Phys. Letters **16**, 165 (1965).
[5] L. Gilly, M. Jean, R. Meunier, M. Spighel, J. P. Stroot, and P. Duteil, Phys. Letters **19**, 335 (1965).

[6] T. Kohmura, Progr. Theoret. Phys. (Kyoto) **33**, 480 (1965).
[7] A. K. Kerman and R. K. Logan, Argonne National Laboratory Report No. ANL-3848, 1964 (unpublished), p. 236.
[8] R. G. Parsons, J. S. Trefil, and S. D. Drell, Phys. Rev. **138**, B847 (1965).
[9] D. S. Koltun and A. Reitan, Phys. Rev. **139**, 1372 (1965).

FIG. 1. Apparatus for the detection of pion double charge exchange. Positive pions produced in the cyclotron enter from the right. Negative pions pass through the analyzing magnet and stop in the range spark chamber. Complete trajectories in the spark chambers are photographed.
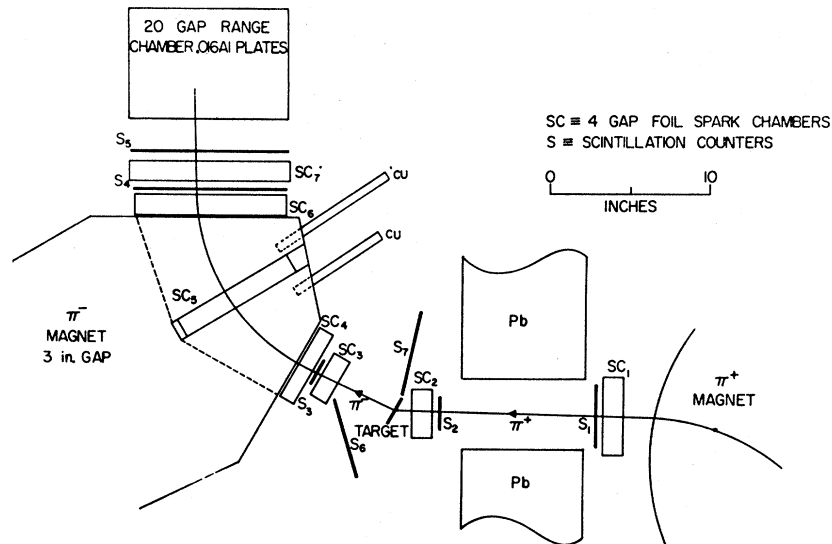
the Coulomb energy difference of initial and final nuclei and the mass difference between neutrons and protons.

The following criteria were used in choosing a target:

(1) The target should have as large a neutron excess as possible.
(2) The nuclear charge of the target should be small enough that the incident pion would penetrate the Coulomb barrier and the produced pion would have enough energy to be readily detected.
(3) Since about 15-g quantities are needed for a target, the substance should occur almost isotopically pure in nature.

Natural vanadium was chosen since it is 99.75% V_{23}^{51}, which has five more neutrons than protons. The Coulomb energy difference for V^{51}-Mn^{51} was estimated to be 15.92 MeV using an empirical expression of Long et al.[10] for $\Delta T_3 = 1$ transitions. Their value was doubled since $\Delta T_3 = 2$ in this experiment. For a 31-MeV incident positive pion this gives a 17.7-MeV outgoing negative pion and a differential cross section of 57.5 μb/sr predicted from the theory of Koltun and Reitan.

In addition to V^{51}, we chose the target Li^7 since it had been observed at CERN to have a forward double-charge-exchange cross section of about 100 μb/sr at 195 MeV.[11] Similar cross sections for Be and Na were one and two orders of magnitude lower. It seemed worthwhile to supplement their measurement with a measurement near 30 MeV. Another group whose work was more concurrent with our own used these same targets at 200 MeV for similar reasons.[12]

Three runs were taken on this experiment. The first allowed us to pinpoint and eliminate some sources of background. In the second, good running conditions were obtained, but no events were seen. One event for each target would have corresponded to a cross section of about 2 μb/sr on V^{51} and about 0.55 μb/sr on Li^7. We reported these initial results at the New York meeting of the American Physical Society.[13] For the third run, we moved the magnet for the outgoing pion closer to the target in order to increase solid angle, and we added a spark chamber halfway through the magnet in order to eliminate uncertainty about spurious events.

II. APPARATUS

Positive pions are produced by the proton beam striking a carbon target within the Rochester 130-in. synchrocyclotron. The pion beam is extracted and focused by the fringe field of the cyclotron and further defined by slits and a lead channel. It is then bent about 60° by a double-focusing magnet. The cyclotron is operated with a stretched beam in order that only one pion track will be present in each photograph. The beam intensity averaged about 1.5×10^4 pions/sec with a duty cycle of over 60%. After passage through the π^+ magnet, the first two scintillation detectors, and the thin-foil spark chambers, the pion beam had a mean energy of 32 MeV with full width at half-maximum (FWHM) of 3.5 MeV. Traverses of the beam showed roughly Gaussian shapes with FWHM of 1.4 in. horizontally and 1.9 in. vertically.

Our final experimental layout is illustrated in Fig. 1. To determine that a pion double-charge-exchange reaction has taken place, one must ascertain that the particle leaving the target is negative and a pion. Many

[10] D. D. Long, P. Richard, C. F. Moore, and J. D. Fox, Phys. Rev. **149**, 906 (1966).
[11] L. Gilly, M. Jean, R. Meunier, M. Spighel, J. P. Stroot, P. Duteil, and A. Rode, Phys. Letters **11**, 244 (1964).
[12] J. Solomon, Proceedings of the Williamsburg Conference on Intermediate Energy Physics, 1966 (unpublished), p. 269.
[13] C. J. Cook, R. L. Burman, and M. E. Nordberg, Jr., Bull. Am. Phys. Soc. **12**, 104 (1967).

spurious positive pions, protons, and electrons had to be eliminated. The trajectory of the particle in a magnet determined its charge and momentum, and its stopping point in a 20-gap spark chamber determined its range. Scintillation detectors registered the arrival of a positive pion and the passage of an outgoing particle. Fast logic circuits triggered the thin-foil spark chambers and the range chamber, in which complete incoming and outgoing trajectories were recorded. The radius of curvature of a particle passing through the magnet can be constructed from the entrance, middle, and exit locations. With the magnetic field measured and known, the momentum of the particle is thus determined. This momentum combined with the range-chamber measurement uniquely determines the identity of the particle.

The electronic logic required an $S_1S_2S_3S_4S_5\bar{S}_6\bar{S}_7$ coincidence as defined in Fig. 1 in order to trigger the spark chambers. It would have been desirable to have had fewer detectors in the detecting system since the energy loss in these detectors puts a low-energy limit on the pions that can be detected. However, removal of any of these detectors from the logic increases the picture-taking rate by an order of magnitude. Detector No. 3 was made as thin as easily feasible (0.030 in.) to reduce multiple scattering which could distort the measurement of momentum and the point of origin in the target. All detectors had measured efficiencies over 95%.

The direction spark chambers were constructed with 0.001-in. Al foil and $\frac{5}{16}$-in. Lucite frames. Each chamber had four gaps, with three ground and two driven foils. The redundancy of gaps was to assure that at least two gaps would spark along a particle trajectory. Most of the time, three or four gaps sparked correctly. The front and back of these chambers had a pressure seal of 0.001-in. foil so each chamber presented 0.007 in. of Al absorber to the particles that passed through normal to the foils. All the spark chambers were filled with 90% Ne and 10% He at just above atmospheric pressure.

The range chamber had 20 gaps and was constructed similarly to the direction chambers except that 0.016-in. Al sheets were used. It was designed to measure the energy of 20-MeV pions to within about 0.5-MeV uncertainty. It was useful in beam surveys as well as in the actual experiment.

The detection system was sensitive to pions with production angles of about 29°. The horizontal angular aperture was about 20°, and the vertical aperture was about 9°. The horizontal focusing properties of the π^- wedge magnet are such that particles diverging from the target come out roughly perpendicular to the range chamber plates. The line connecting the center of the target of the No. 3 counter is normal to the entrance of this magnet. By having near normal incidence and exit of the pions, vertical focusing from the magnet fringe field is negligible. Also, the pions cross the slot

in the magnet in a near normal manner, which minimizes vertical focusing or defocusing there.

The π^- magnet was calibrated with current-carrying wires. Close agreement between simulated trajectories made with current-carrying wires under tension, and trajectories constructed from the measured effective magnetic field was obtained. In these measurements the radii were reproducible within a range of about ±2.5% of their mean value.

III. EXPERIMENTAL PROCEDURE

The detectors were initially adjusted in the direct pion beam. Timing and attenuation curves were taken and conservative operating points chosen. Pulse-height spectra were recorded for the pion beam and for the Bi^{207} internal conversion electrons. The π^- magnet and detectors were then put in their running position. With all magnetic fields on, the pulse-height spectra for the Bi^{207} were again taken and compared with the previous spectra. The detector gains were not affected by the magnetic fields. Many times during the run, detector gains were checked with sources and found to be stable within about 1 dB.

In order to test the apparatus with a π^- beam, the cyclotron and the π^+ magnet fields were reversed, thus reversing the sense of rotation of the internal proton beam, so that negative pions produced from the internal target would be conducted through the same beam channel. This π^- beam was degraded and scattered through the detection system by the vanadium target to which $\frac{3}{8}$-in. of Al had been attached, which simulates by ionization loss the expected energy loss in the double-charge-exchange reaction. Timing and threshold discrimination curves were taken with these scattered pions. The timing was exactly as before. The critical counters, Nos. 3, 4, and 5, which had double magnetic shields, maintained their original gain within 1 dB. The No. 1, 2, 6, and 7 counters all intercepted enough of the direct beam that their timing and threshold settings could be easily checked at any time. Three hundred pictures of negative pions were taken with the π^- magnet at a mean magnetic field of 6.08 kG. These pictures were later used to test the calibration and dispersion of this detection system.

The beam was returned to positive pions and the experiment was run with a V^{51} target 0.635 g/cm² thick and 2 in. square, and with the π^- magnet set at 7.06 kG. It was soon evident that there was a significant number of electrons produced through single-pion charge exchange followed by conversion of a decay γ ray into an electron-positron pair. In earlier runs, this background was not identified with certainty. With the spark chamber in the middle of the π^- magnet, negative particles could be clearly identified. Also, protons produced by pion capture and positive muons produced by decay of the incident beam could not be mistaken for negative pions. There were many negative particles

TABLE I. Statistics of third run.

Target	π^--magnet $\langle B \rangle$ (kG)	1·2 counts	Pions on target	Pictures taken
V^{51}	5.83	5.23×10^9	4.63×10^9	7936
V^{51}	7.06	5.40×10^9	4.78×10^9	6368
Li^7	5.83	2.43×10^9	2.15×10^9	4276
Li^7	7.06	2.31×10^9	2.04×10^9	2935

with short radius that missed the range chamber. To be sure that these were not pions, an equally long run was taken with the π^- magnet set at 5.83 kG. In this reduced field, these particles would not be bent as much and should strike the range chamber. This did not decrease our threshold for low-energy pions, which was determined by ionization losses and corresponded to a pion energy of 8 MeV. Rather, the main result of running at lower magnetic fields was to further separate the pion radius-range curve from the electron background.

Two similar runs were made with a Li^7 target 0.675 g/cm² thick. The runs are summarized in Table I.

IV. DATA REDUCTION

A. Film Scanning

The film was projected and scanned three times for negative particles passing through the π^- magnet. The large majority of spark triggers are due to random coincidences and not to a single particle passing through the system. The resulting spark pattern is chaotic and disconnected so these pictures can be scanned and discarded quickly. About one-fifth of the photographs were of a proton from pion capture in the spark-chamber frame. These were reassuring because they indicated throughout the experiment that the counters were set correctly and the spark chambers were sparking efficiently. Many photographs were of electrons that travel completely through the range chamber. In some of these cases, a positron track was also seen in spark chamber No. 3. For negative particles, the projected radius of curvature and production angle were measured and the stop gap in the range chambers was noted. It was also checked that the mirror views of the trajectories were compatible, that the particle had its origin in the target at the intersection of the beam with the target, and that the incident particle followed a straight path down the beam channel and was not produced off the wall. Also, any obvious production of an electron pair anywhere in the apparatus was noted. The projected radius of curvature was measured to $\pm \frac{1}{8}$ in. with a template; the projected image was about two-thirds the size of the actual apparatus.

Those negative particles that had their origin in the target and were not obviously from an electron pair were plotted on a radius versus range-chamber stop-gap curve where they were compared with the expected radius versus range curve for a pion.
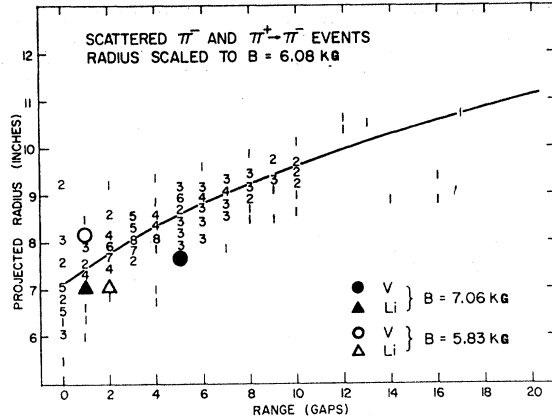
FIG. 2. Radius-range plot for events and scattered pions. The four apparent double-charge-exchange events are plotted together with the calibration points obtained with a negative pion beam.

Four negative particles which appeared to definitely stop in the range chamber fall within an inch of the projected radius from the expected pion curve and are considered to be negative pions from double charge exchange. The projected radii of these four events are scaled for a common magnetic field of 6.08 kG and are displayed on a range-radius plot (Fig. 2) together with the scattered negative pions which were used to calibrate the detecting system. The events fall within a band comparable to that occupied by the known negative pions.

The number of negative particles of various categories observed in the 5.83-kG V^{51} run is typical of all the runs and is displayed in Table II. These do not form a complete set of mutually exclusive types.

B. Possible Electron Contamination

Estimates show that the chance of an electron simulating a pion is small. An 8-MeV pion in the π^- magnet, which is about the minimum detectable energy for this experiment, has a momentum of 48.5 MeV/c. An electron simulating this pion would have this same momentum but would have a kinetic energy of roughly 48 MeV. The mean range for such an electron in Al is 21 g/cm².[14] Were this electron to lose 90% of its energy

TABLE II. Some scan results for V^{51} target with the π^- magnet at $\langle B \rangle = 5.83$ kG.

Type	Number
Pictures taken	7936
Negative particles in π^- magnet	197
Negative particles that hit target but are not clearly half of a pair	70
Negative particles that clearly missed target	51
Electron pairs produced before target	47
Electron pairs produced in target	17
Double-charge-exchange events	1

[14] W. Heitler, *The Quantum Theory of Radiation* (Oxford University Press, London, 1954), 3rd ed.

by bremsstrahlung, its mean residual range is still 3.11 g/cm². Thus, an electron that had adequate momentum to simulate a pion should have so much energy that it could lose a large portion of its energy to bremsstrahlung and still travel completely through the range chamber and not be mistaken for a pion.

It is possible for an electron to scatter approximately 90° from a nucleus, leave the range chamber without leaving a track, and be interpreted as a pion that has come to the end of its range. Using the Coulomb cross section, a conservative estimate of their number in this experiment is 0.04 electrons.

For an electron-electron collision without bremsstrahlung, one electron must come out of the collision with more than half of the incident energy and continue close to the initial direction of motion; and, thus, it should have enough residual range to look like an electron rather than a pion.

From these arguments, we conclude that there is at least a 95% probability that our events are real. If some or all of our events are not real, then the cross sections calculated later are good only as upper limits.

C. Sensitivity of the Detection System

The following procedure was used in calculating the mean acceptance solid angle for the detection system.

(1) The acceptance solid angle for pions with various radii of curvature and origins on the target was calculated from the geometry of the system. The vertical aperture is determined by the magnet gap and the horizontal aperture by the No. 3 detector and the range chamber.

(2) The average solid angle for pions of various radii for the whole target was obtained by integrating these expressions over the target using the beam spatial distribution as the weighting factor.
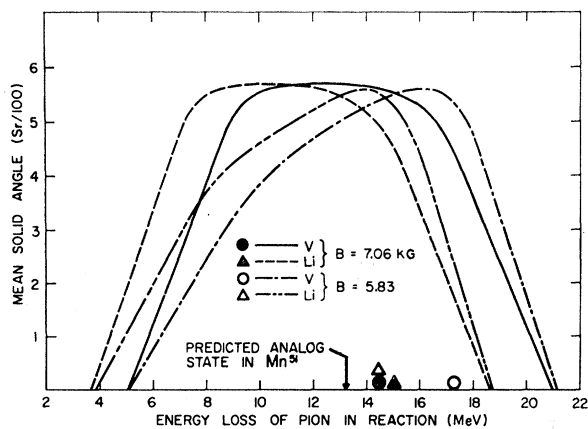
FIG. 3. Sensitivity versus energy loss in reaction. The high cutoff is caused by the outgoing negative pion having insufficient energy to pass through the scintillation detectors and spark chambers. The low cutoff is caused by the outgoing negative pion of high momentum missing the range spark chamber.

(3) Assuming an incident pion of 32 MeV, the relationship between energy and momentum for a pion, and the relationships between radius of curvature and momentum for our experiment, the solid-angle versus radius-of-curvature curve was translated into solid-angle versus energy loss in the target curves. For large ΔE, the pion has insufficient energy to penetrate all the counters; and, for small ΔE, the pion will travel through more than 18 gaps of the range chamber and will not be considered a candidate for charge exchange.

(4) Since the beam is polyenergetic, the solid-angle versus energy loss in target curves should be somewhat smoothed and spread out from those with a monoenergetic beam. To construct such a curve, the beam was considered composed of components of 30, 32, and 34 MeV with relative strengths of 1:2:1.

(5) The solid angle versus energy loss in target curves were transformed into solid angle versus energy loss in reaction curves (Fig. 3). The energy loss in the target is due to both ionization and reaction losses. To calculate how much is due to ionization, it was assumed that the incident energy is 32 MeV, that the pion suffers ionization loss for half the target, reacts, and then continues to lose energy by ionization through the rest of the target. A 32-MeV pion is degraded to 31 MeV after it has traveled through half the V target and is degraded to 30 MeV halfway through the Li target. These energies at the center of each target are taken as the nominal energies for the experiment.

(6) The events are displayed in Fig. 3. The energy loss was obtained using the same assumptions as in step (5). Considering the energy spread in the beam (FWHM of 3.5 MeV), the actual energy loss could differ by several MeV from the displayed values.

V. CROSS SECTIONS AND CONCLUSIONS

With only two events for each target, the dominant limitation on the accuracy of our cross-section measurements is statistical. This low number mandates the use of the Poisson distribution, which is skewed toward larger numbers. Unfortunately, the two events coupled with our energy resolution do not give a complete enough π^- energy spectrum to tell with certainty whether the reaction for vanadium was

$$V^{51} + \pi^+ \to Mn_{analog}^{51*} + \pi^-$$
$$\text{state}$$

or

$$V^{51} + \pi^+ \to Cr^{50*} + p + \pi^-.$$
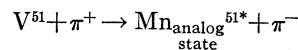
The two events do appear to be displaced toward the high-energy-loss region of the sensitivity curve and do not center on the predicted analog state. The average of their energy loss is 16 MeV rather than the predicted 13.3 MeV.

Weighting the two events with the inverse of the solid angle at their respective values of energy loss, we find

$$(d\sigma/d\Omega)_{29°}{}^{V^{51}} = 0.52_{-0.19}^{+0.71} \ \mu b/sr.$$

This measurement of cross section to the energy-loss interval 7 to 19 MeV (which covers the predicted isobaric analog state) is less by a factor of 100 than the cross section predicted by Koltun and Reitan.[9] It was this theory which our experiment was most specifically designed to test.

Our result is comparable with Kohmura's calculation[6] of a total cross section of 15 μb for O^{18} at 10 MeV, if we assume his angular distribution is isotropic. However, the difference in the target and energy possibly makes such agreement fortuitous and not really significant.

Comparison of our results with the theory of Kerman and Logan[7] is complicated by the fact that we do not really know what their theory implies for the differential cross section we have measured. We have an interpolated value of about 1 μb for their total cross section. We know that their angular distribution is not isotropic[15] but do not know its detailed shape. Were we to consider their differential cross section equal to $1/4\pi$ μb/sr, we would conclude that their calculations were low by a factor of about 5. If their angular distribution is peaked forward, their calculations could well be in accord with our measurements. It should be noted that their calculations were done with the intent to set lower limits on double-charge-exchange cross sections. Our measurement is more believable for setting an upper limit than a lower limit on this cross section. That is, if our two events were actually spurious, then our lower limit would be wrong, but our upper limit would still be of value.

The calculation of Parsons et al.[8] for O^{18} is about a factor of 10 lower than our measured cross section for V^{51}. Since there are 10 neutron pairs in V^{51} available for double charge exchange and only one such pair for O^{18}, there may be some grounds to consider these comparable results.

Comparison of our results with other experiments is complicated by the fact that other experiments have been performed at much higher energies.

The first observation of double charge exchange was by the Russian group of Batusov, Bunyatov, Sidorov, and Yarba.[16] This was a byproduct of a study of pion production in nuclear emulsion when bombarded with 250–300-MeV negative pions. Some of the produced positive pions had double charge exchanged to negative pions. This group then irradiated emulsions with 80-MeV positive pions and obtained 30 double-charge-exchange events for positive pions with energies ranging from 30 to 80 MeV. No events were seen for pions with energy less than 30 MeV. The total cross section was 400 μb.

Other work by this group has been done on Be, C, Al, and Pb, using nuclear emulsions for particle detectors.[17–19] Their curves show a marked increase of cross section with energy. It is quite difficult to extrapolate their cross section versus energy curves to 30 MeV, but our rather low cross section is compatible with their curves.

The double-charge-exchange reaction for Li^7 is expected to be to many-body final states, being either $Li^7 + \pi^+ \rightarrow He^4 + p + p + p + \pi^-$ or $Li^7 + \pi^+ \rightarrow He^3 + n + p + p + p + \pi^-$. The two events for lithium are near the high-energy-loss edge of the sensitivity curve, their average energy loss being 14.8 MeV. For the differential cross section we find

$$(d\sigma/d\Omega)_{29°}{}^{Li^7} = 0.165_{-0.060}^{+0.225} \ \mu\text{b/sr}.$$

This is at least an upper limit on the differential cross section for pion energy loss from 7 to 17 MeV. It is possible that pions with larger energy loss are being produced but are not detectable by our apparatus. This is suggested by the incidence of the two events at the high-energy-loss edge of our sensitivity curve. Our differential cross section at 30 MeV is a factor of 600 smaller than that measured by the CERN group at 195 MeV.[11]

ACKNOWLEDGMENTS

[15] A. K. Kerman (private communication).

[16] Yu. A. Batusov, S. A. Bunyatov, V. M. Sidorov, and V. A. Yarba, Zh. Eksperim. i Teor. Fiz. 46, 817 (1964) [English transl.: Soviet Phys.—JETP 19, 557 (1964)].

[17] Yu. A. Batusov et al., Yadern. Fiz. 1, 383 (1965) [English transl.: Soviet J. Nucl. Phys. 1, 271 (1965)].

[18] Yu. A. Batusov et al., Yadern. Fiz. 3, 309 (1966) [English transl.: Soviet J. Nucl. Phys. 3, 223 (1966)].

[19] Yu. A. Batusov et al., Yadern. Fiz. 5, 354 (1967) [English transl.: Soviet J. Nucl. Phys. 5, 249 (1967)].